RARE EARTH BEARING-MINERALS OF THE PETACA DISTRICT, RIO ARRIBA COUNTY, NEW MEXICO

MICHAEL N. SPILDE[1], STEVE DUBYK[2], BRIAN SALEM[3], AND WILLIAM P. MOATS[4]
[1]Institute of Meteoritics, MSC03-2050, University of New Mexico, Albuquerque, NM 87131 (mspilde@unm.edu).
[2]1828 Quiet Lane SW, Albuquerque, NM 87105, [3]PO Box 27, Tijeras, NM 87059, [4]8409 Fairmont Drive NW, Albuquerque, NM 87120

Abstract—Ten pegmatites were sampled across the Petaca District of northern New Mexico. Samples were analyzed by electron microprobe to identify composition and mineral type and to determine the presence of rare earth elements (REE). Monazite-(Ce) is present throughout the district and contains significant enrichment of Th, in addition to Ce and other light REE. Thorite and xenotime were found to be enriched in moderately heavy REE. Zircon, while not high in REE, contained significant Hf. Samples of Y-REE-Ta-Nb-Ti oxides were analyzed and then classified using statistical analysis into polycrase-(Y), euxenite-(Y), and samarskite-(Y). Polycrase is a new mineral for the state. Samples of columbite-tantalite group minerals were analyzed and found to be columbite-(Mn). Based on the mineralogy of these pegmatites, they can be classified as NYF pegmatites and are likely derived from shallow A- or I-type granite bodies not yet exposed in the region.

INTRODUCTION

The Petaca District, located in northern New Mexico, has had a long history of muscovite mica production from granitic pegmatites, which has been described in some detail by Sterrett (1923), Just (1938), and Jahns (1946, 1974). These authors have also noted the presence of several rare minerals that occur in the pegmatites and were occasionally recovered as a by-product of mica mining. These minerals include monazite-(Ce) and other minerals that contain rare earth elements (REE) but have received little attention from the scientific community. Here we present the results of a microprobe study of Y-REE-Ta-Nb-Ti oxide minerals as represented by samples recently collected from several properties in the Petaca District. This study was conducted with the goal of characterizing the concentration and distribution of REEs and to identify new instances or confirm prior reports of the REE-bearing minerals present in these pegmatites. An additional goal of this paper is to examine the origin of the Petaca pegmatites based on the mineralogy of the deposits.

LOCATION AND HISTORY

The Petaca District lies west of the Rio Grande near the eastern margin of Rio Arriba County, in rugged, forested country of the Tusas Range (Fig. 1). The district is accessed by US Forest Service roads whose condition ranges from good to poor and unpaved. The roads extend from New Mexico state highways 111 and 519, the main routes leading from the village of La Madera northward to Vallecitos and Petaca. The district occupies a broadly curving belt, varying from 1 to 4 ½ miles wide and about 15 miles long, and extends from Kiawa Mountain, southeast of Hopewell Lake, southeastward and southward to the village of La Madera (Jahns 1974). The mined and prospected pegmatites lie between the Tusas and Vallecitos Rivers, mainly on Jarita Mesa and in the canyon country that flanks this mesa on the east (Fig. 1).

Pegmatites in the district were mined for sheet and scrap mica from about 1870 through the end of World War II (1945), with some mining continuing at the Globe mine into the late 1950's and perhaps as late as 1965. Jahns (1946) reports that mica may have been recovered from mines at the Cribbenville town site (abandoned) as early as the 17th century, which may represent the earliest systematic effort to mine sheet mica in the United

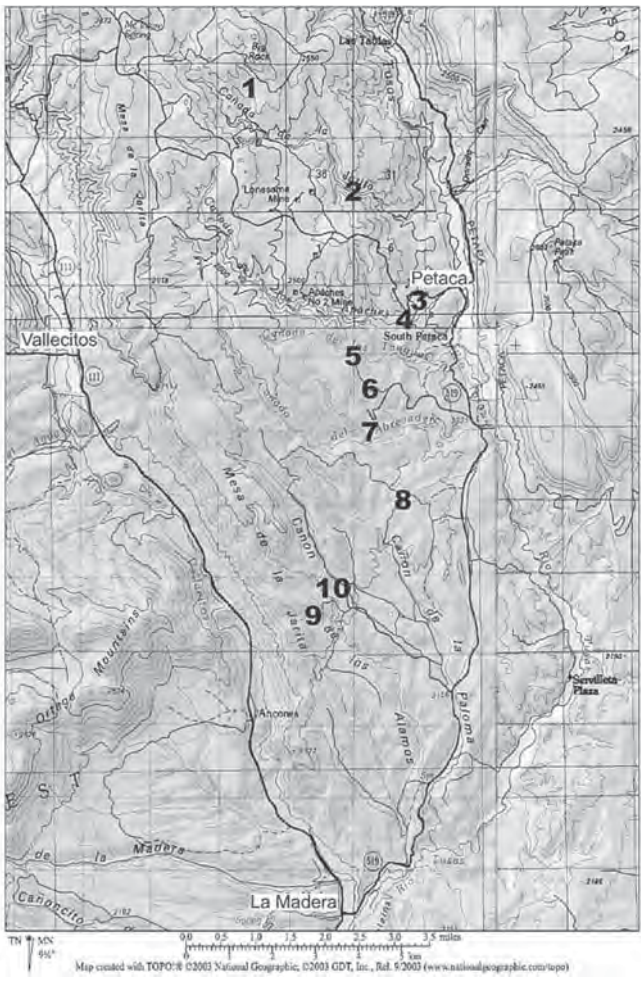

FIGURE 1. Map of the Petaca mining district. Approximate locations of the pegmatites sampled in this study are shown: 1, Alma; 2, North Star; 3, Coats; 4, Bluebird; 5, Fridlund; 6, Freetland; 7, Nambe; 8, La Paloma; 9, Alamos Canyon ; 10, Globe.

States. The Petaca District is estimated to have produced about 250,000 pounds of sheet, scrap, and punch mica (Jahns 1946). Mining claims have recently been located on some of the pegmatites, presumably because of the high demand for REEs as raw materials for the technology industry. Finally, a brief assessment by the U.S. Geological Survey of the economic potential of rare-earth mineralization at the Petaca District was recently presented by Long and others (2010).

GEOLOGY OF THE PEGMATITES

The geology of the Petaca District pegmatites has been described in detail by others (Jahns, 1946; Just, 1937; Wright, 1948). Only a brief summary is presented here, which draws heavily from Jahns (1946). The Petaca District pegmatites are classified as rare element pegmatites, as defined by London (2008), and occur in 5 major geographical groups. Extending from north to south, these are the Kiawa, Persimmons Peak-Las Tablas, La Jarita-Apache, Cribbenville, and Alamos groups. A few outlying pegmatites constitute the rest of the district. U-Pb dating (zircon) places the age of crystallization of the pegmatites at approximately 1400 Ma (Koning et al., 2007). The pegmatites form dikes, sills, pods, and irregular bodies that intrude Paleoproterozic metasedimentary and metavolcanic rocks of the Vadito Group (Koning et al., 2007; Scott et al., 2010). The Precambrian terrane that hosts the pegmatites is surrounded and locally covered by a veneer of volcanic and volcaniclastic rocks of Cenozoic age.

In general, the pegmatites trend west-northwest to west-southwest, and dip steeply north or south. A border zone, a wall zone, usually one or more intermediate zones, and a core zone generally comprise the larger pegmatites, and replacement bodies of albite ± muscovite and fracture fillings of quartz ± albite are common. The pegmatites are composed chiefly of microcline (perthite), quartz, albite, and muscovite, which occur as medium to coarse-grained aggregates with granitoid textures in wall zones, and as large or giant anhedral to euhedral crystals in intermediate zones. However, only one or two minerals typically dominate the intermediate zones. The pegmatite cores are usually composed of quartz, or less commonly quartz + microcline. Spessartine, fluorite, columbite-tantalite, monazite-(Ce), beryl, ilmenite, and bismutite are the common accessory minerals, which, except for beryl, occur mostly as scattered crystals or small anhedral masses in quartz, in intermediate or replacement zones rich in albite ± muscovite, or in fracture fillings. Beryl is reported by Jahns (1946) as occurring chiefly in the wall zones of the pegmatites, but has been observed in all zones. Amazonitic K-feldspar is locally common in some areas of the district, particularly in the vicinity of the Mica Lode and Vestegard deposits.

PREVIOUS WORK

REE-bearing minerals previously reported from the Petaca District include those from the monazite, euxenite, columbite, gadolinite, aeschynite, fergusonite, and samarskite groups. Of these minerals, only monazite is easy to identify in hand specimens. Chemical analyses of monazite specimens from Petaca pegmatites have been previously published by Heinrich and others (1960) and Modreski (1986). Based on these earlier studies, as well as this work (Appendix 1), cerium is the dominant REE. Thus, monazite from the Petaca District is more properly identified as monazite-(Ce) under modern nomenclature.

Northrop (1959) lists euxenite and yttrotantalite as being present in the Petaca District based on unpublished letters authored by Ming-Shan Sun and Jahns in 1956 and 1957, respectively. Northrop (1959) further indicates that the identifications for gadolinite and aeschynite should be considered tentative (Northrop, 1959; Hess and Wells, 1930). Based on the circumstances surrounding these identifications, it seems apparent that additional work was needed to confirm whether euxenite, yttrotantalite, gadolinite, and aeschynite actually occur in the Petaca District, although according to Northrop (1959), Jahns' letter indicated the identification for yttrotantalite was without doubt. In his letter, Jahns reports that specimens of yttrotantalite were found at the Apache, Coats, Capitan, and White mines, suggesting a widespread distribution for this mineral in the Petaca District.

Based on chemical analyses, samarskite and fergusonite were identified in samples obtained from the Fridlund mine (Hess and Wells, 1930; Wells, 1928). The dominant REE in these minerals cannot be determined from these data, so the exact mineral species within the samarskite and fergusonite groups that are represented by the Fridlund samples are not known.

PRESENT STUDY

Methods

Samples of REE-bearing and Ta-Nb minerals were collected across the district from Alma, Alamos, Bluebird, Coats, Fridlund, Freetland, Globe, La Paloma, Nambe, and North Star pegmatite mines (Figure 1). Initial identification and location of the mineral samples was done in the field using radiometric detectors, since many of the REE minerals exhibit varying degrees of radioactivity. Samples were tentatively identified using energy dispersive X-ray analysis (EDX) on a JEOL 5800LV scanning electron microscope (SEM) at the Institute of Meteoritics/Department of Earth and Planetary Sciences at the University of New Mexico in Albuquerque, NM. Representative samples, selected for detailed analysis, were mounted in epoxy and polished using a series of silicon carbide, diamond, and alumina grits for electron microprobe (EMP) analysis. These samples were examined in a JEOL 8200 Superprobe also at the Institute of Meteoritics at 15 kV with beam currents between 10 and 100 nA. Natural mineral standards were used for calibration of most elements except the REEs where synthetic REE-phosphates were used. X-ray counting times ranged from 10 to 60 seconds, depending on concentration, and matrix corrections were done using the ZAF method (Goldstein et al., 2003).

Results and Discussion

Several new minerals were confirmed for the district, including euxenite-(Y), samarskite-(Y), polycrase-(Y), xeneotime-(Y),

and microlite. However, some minerals such as yttrotantalite, fergusonite, gadolinite and aeschynite were not found and could not be confirmed. Appendix 1 lists representative compositions of minerals analyzed during this study.

Phosphates: Monazite and Xenotime

Probably the most abundant of the REE-bearing minerals in the Petaca District, monazite-(Ce) [(Ce, La, Nd, Th)PO_4] has been found as reddish brown or salmon-colored, blocky masses and crystals weighing up to a half kilogram. Heinrich et al. (1960) noted that the mineral had been found in 83 percent of the deposits examined at Petaca where it was closely associated with columbite, samarskite and fluorite in albitized parts of the pegmatites. Backscattered electron imaging of our samples revealed that monazite is often riddled with inclusions of thorite, which are surrounded by a halo of cracks caused by radiation damage induced by the Th-rich inclusions (Figure 2A). In addition, some monazite exhibits zones along fractures in which the monazite has been invaded by xenotime (YPO_4) and other Th- and REE-bearing phosphate compositions (Figure 2B). All of the monazite analyzed in this study contains some concentration of ThO_2, ranging from a few wt% to as much as 15 wt% in a sample collected at the Coats pegmatite. However UO_2 and PbO content is always less than 1 wt%, although PbO of 1% was noted in the sample from the Coats pegmatite. Monazite-(Ce) from the Petaca pegmatites contains predominantly light rare earth elements (LREE: La to Eu), dominated by Ce, although other LREE may also be present. For example, both La_2O_3 and Nd_2O_3 are as high as 13 wt% in monazite from the Globe and Fridlund mines. Figure 3 shows the chondrite-normalized REE distribution for the minerals analyzed in this study. Monazite strongly prefers the LREE, whereas xenotime is enriched in the HREE, especially the lower end of the HREE range (i.e. Gd to Ho).

Xenotime-(Y) is a rare phosphate mineral found in the Petaca district. Coarse crystals of xenotime were not found during this study; instead it was observed as vein-like alterations of monazite and as sub-millimeter inclusions in monazite and Y-rich fluorite. Xenotime-(Y) inclusions and veinlets contain significant heavy REE (HREE: Gd to Lu), particularly Dy_2O_3 as high as 15-23 wt%, substituting for Y_2O_3 in the Fridlund and Coats samples. Because Y behaves as a HREE, these elements will substitute into the Y-site (Ercit, 2005). However, at La Paloma, HREE was low, but significant ThO_2 (14.5 wt%) was found in the xenotime. Additionally most of the monazite and xenotime samples contained some level of As_2O_5. The substitution of vanadates, arsenates and silicates for phosphate reaches its highest levels in xenotime. In samples from the Fridlund and Coats mines, xenotime contained over 1 wt% As_2O_5. Furthermore, we note that there is a continuous series between phosphate and silicate in monazite, xenotime and thorite at several of the Petaca pegmatites. This substitution in the anion site, shown in Figure 4, is most notable in samples from the Coats Mine.

Thorite and Zircon

A kilogram mass of yellowish-brown, pulverulent (i.e. powdery) thorite ($ThSiO_4$) was found at the Coats mine. The composition of this sample was highly variable and contained significant amounts of phosphate in addition to silicate (Figure 4). The PO_4-rich material occurs in veinlets scattered throughout the larger thorite sample. The veinlet material is probably what used to be known as "cheralite" [(Ce, Th, Ca)(Si, P)O_4], although that mineral has been discredited by the International Mineralogical Association and is now considered to be "Ca-rich monazite." Thorite also occurs as inclusions in monazite at the Coats, Fridlund, La Paloma and North Star deposits. Inclusions range from individual mm-size to swarms of micrometer-size inclusions. The larger ones usually induce fracturing in the monazite as a manifestation of radiation damage (Figure 2A). In addition, the thorite samples analyzed in this study always contained some As_2O_5, PO_4 and V_2O_5 (Fig. 4), along with a few wt% of REE.

Zircon ($ZrSiO_4$) was found at La Paloma occurring as mm-sized black crystals in quartz, associated with samarskite and bismutite (Figure 2C). Although zircon is low in REE, it is notably high in HfO_2, containing up to 6 wt%.

(Y, REE, Th, U) (Ta, Nb, Ti) Oxides

The REE-bearing oxides may be separated into two main divisions on the basis of their formulas: AB_2O_6 and ABO_4. In each case, the A-site contains Y, REE, U, Th, Na, Ca, and Fe and the B-site contains Ta, Nb and Ti. The AB_2O_6 division may be further defined structurally as the aeschynite group, polycrase-euxenite group, and the pyrochlore group, and the ABO_4 division is subdivided into the samarskite and fergusonite groups. Within the aeschynite group, the name is derived from the major A-site cation, such as aeschynite-(Ce) [$Ce(Ti, Ta, Nb)_2O_6$] or aeschynite-(Y) [$Y(Ti, Ta, Nb)_2O_6$]. Members of the polycrase-euxenite group include euxenite-(Y) [$Y(Nb, Ti)_2O_6$], tanteuxenite [$Y(Ta, Nb, Ti)_2O_6$], polycrase-(Y) [$Y(Ti, Nb)_2O_6$], and uranopolycrase [$(U, Y)(Ti, Nb)_2O_6$]. The aeschynite structure shows a preference for larger A-site cations than the euxenite structure; thus, aeschynite group minerals have a higher LREE : HREE ratio than euxenite-group minerals (Ewing 1976).

The pyrochlore group has the general formula $A_{2-x}B_2(O,OH)_6(O,F,H_2O)_{1-y}$ and is divided into three subgroups: the betafite subgroup with $2Ti \geq (Ta + Nb)$ at the B-site, and the pyrochlore and microlite subgroups, in which $(Nb + Ta) > 2Ti$ and $Nb > Ta$ (pyrochlore) or $Ta \geq Nb$ (microlite). A wide variety of monovalent to trivalent cations are possible at the A position, resulting in a high number of end members (Ercit, 2005). The most important members known to occur in granitic pegmatites are pyrochlore [$(Ca,Na)_{2-x}Nb_2O_6(O,F,H_2O)_{1-y}$], betafite [$(Ca,Na)_{2-x}Ti_2O_6(O,F,H_2O)_{1-y}$], and microlite [$(Ca,Na)_{2-x}Ta_2O_6(O,F,H_2O)_{1-y}$].

The second division of the Y-REE-Ta-Nb-Ti oxides is the ABO_4 formula, and samarskite and fergusonite are the two important groups in this division. The main member of the samarskite

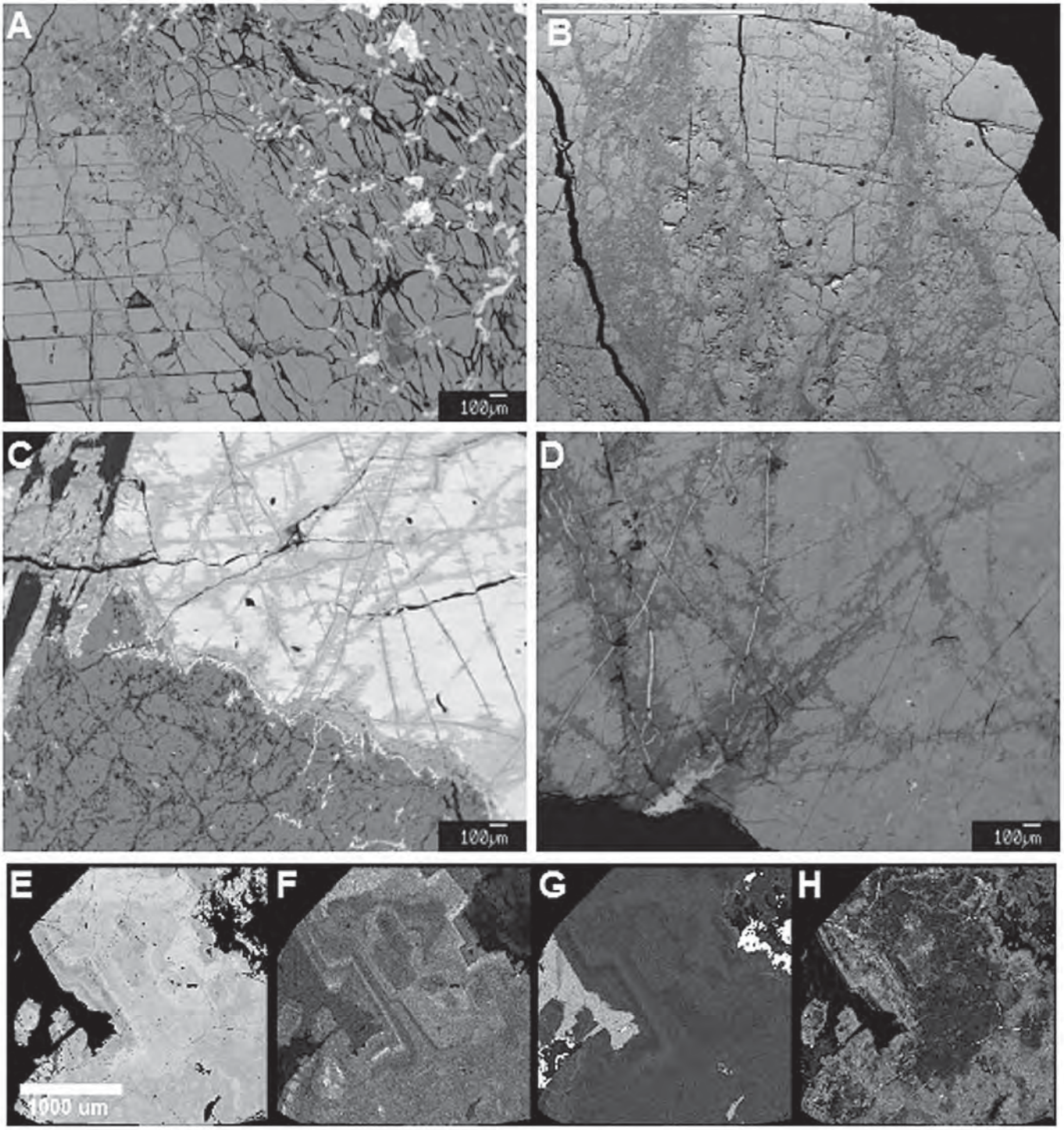

FIGURE 2. Backscattered electron (BSE) micrographs of various minerals from Petaca pegmatites. (A) Thorite inclusions (white) in Coats monazite (medium gray). Compare cleavages in the unaltered monazite at the left with the shattered appearance in the inclusion-rich region on the right. (B) Xenotime alteration veinlets (dark gray) in monazite from the Fleetland pegmatite. Scale bar is 1 mm. (C) From La Paloma pegmatite, dark gray zircon (below) associated with samarskite (light and medium gray) above. The medium gray areas are alteration regions along fractures. (D) Samarskite (medium gray) with pyrochlore (dark) and uranpyrochlore (light) veins from the Fridlund Mine. (E-H) BSE image and X-ray maps of complex compositional zoning in polycrase from the Bluebird deposit. (F) Uranium map. (G) Tantalum map. (H) Calcium map.

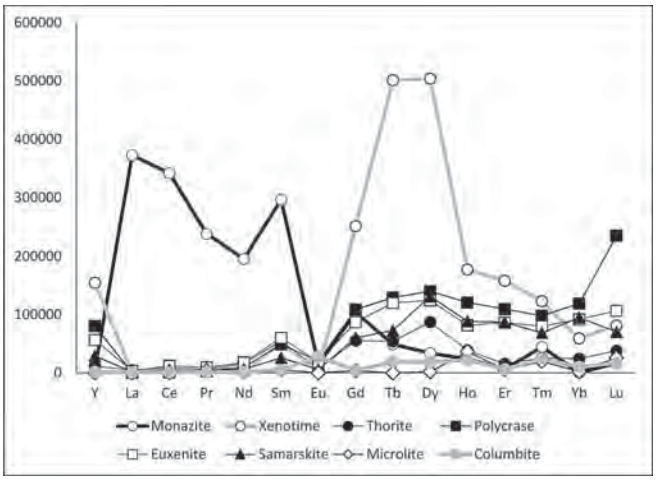

FIGURE 3. Chondrite-normalized REE patterns of average mineral compositions of samples analyzed from the Petaca district. Vertical axis is the ratio of elemental concentration in the mineral to that in type CI chondrite values from Anders and Grevesse, 1984.

group is samarskite-(Y) [(Y,Ca,Fe)NbO_4]. In the general ABO_4 formula for the fergusonite group, the A-site contains Y and REE, and the B-site, Nb and Ta.

Of the 10 pegmatites sampled for "suspect black oxides," Y-REE-Ta-Nb-Ti minerals were found in six of them, but only Bluebird, Fridlund, and La Paloma provided coarse specimens, where they occurred as masses of dark brown to black, glassy minerals up to several cm in diameter. In addition, minute inclusions of Y-REE-Ta-Nb-Ti minerals were found in columbite and other minerals at Alma, Nambe and North Star. Occupancy of the A and B cation sites for these samples is shown in Figure 5. The Bluebird samples tend to form their own cluster with low Th+U and high Y+REE for the A-site chemistry. The B-site is more distributed and shows two main branches, one with extensive solution between Nb and Ti representing polycrase-euxenite-samarskite-aeschynite, and another between Nb and Ta, representing the pyrochlore group. The REE distribution in Fig. 3 indicates that while the LREE partition into monazite, the Y-REE-Ta-Nb-Ti oxides strongly prefer the HREE. Of these, Dy_2O_3 and Yb_2O_3 are often the most abundant.

The Y-REE-Ta-Nb-Ti oxide minerals examined in this study can be highly variable in composition over short distances, with complex zoning. Alteration from one mineral to another has also occurred along grain boundaries and fractures. Figures 2E, 2F and 2G show maps of complex zoning in a polycrase crystal. This type of zoning reflects changes in the composition of the pegmatite fluid during primary growth of the crystal. Late enrichment of tantalum in the late stages of pegmatite crystallization resulted in Ta-rich minerals (columbite-tantalite and microlite) forming around the margins of the polycrase (Fig. 2G), extending from the existing AB_2O_6 structure. Such mineral overgrowth is not uncommon in the late-formed zones of pegmatites, for example wodginite [Mn(SnTa)Ta_2O_8] overgrowths on tantalite (Spilde and Shearer, 1992). In addition to primary zoning, secondary alteration by late pegmatitic fluids further complicates the picture. The map in Fig. 2H suggests a late enrichment of Ca in the outer portion of the polycrase sample. Direct alteration by late fluids is apparent in Fig. 2D where pyrochlore replaces samarskite along fractures, the result of infiltration of fluids rich in U, Ta, and Ca.

Differentiating between Y-REE-Ta-Nb-Ti oxide minerals is hampered not only by the complex chemistry of the minerals, but also by the fact that they are often metamict and display weak or no X-ray diffraction patterns. Furthermore, gross similarity between mineral formulae (e.g. samarskite vs. euxenite vs. fergusonite) adds to the confusion (Ercit, 2005). Ewing (1976) used a statistical approach to classify the Y-REE-Ta-Nb-Ti oxides; Ercit (2005) further refined the technique using principle component analysis (PCA). We take the same approach, using a three-group statistical model (Aabel™, Gigawiz Software, Inc.). The 11 variables used for PCA were Na, Ca, Pb, (Fe+Mn), Y, LREE, HREE, (U+Th), Ti, Nb, and Ta. The results of the classification are shown in Figure 6. A large cluster of the analyses falls within the polycrase field, while smaller groups fall out in the euxenite, samarskite, and pyrochlore fields. The upward sloping vector from polycrase toward samarskite indicates an exchange of HREE for LREE and the downward sloping vector from samarskite toward pyrochlore is the result of the addition of Ca and also probably hydration, although this latter influence was not directly measured.

The classification scheme used points out that most of the Y-REE-Ta-Nb-Ti oxide minerals analyzed in this study fall within the polycrase-euxenite group, with fewer specimens in the samarskite group. This may represent a sampling bias, and certainly more analyses of samples from elsewhere in the district remain to be done to provide better statistical representation. However, these results yield some interesting discussion points. For example, polycrase has not been previously reported in the Petaca district and there is only one report of euxenite being found; most of the reported Y-REE-Ta-Nb-Ti minerals have been labeled as

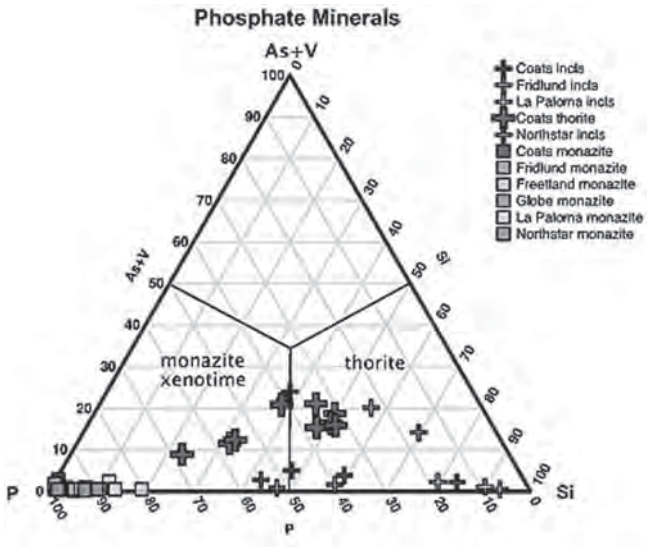

FIGURE 4. Composition of monazite, xenotime and thorite in the (As+V)-P-Si ternary diagram (atomic proportions).

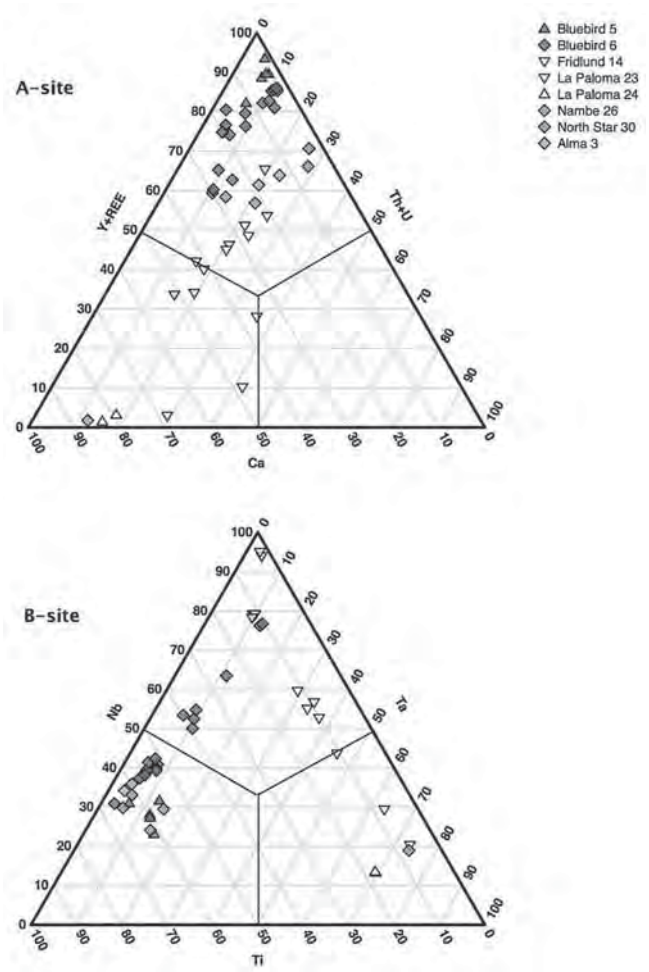

FIGURE 5. Composition of AB_2O_6 and ABO_4 minerals in the (Y+REE)-Ca-(Th+U) ternary diagram (atomic proportions) for the A-site and Nb-Ti-Ta ternary for the B-site.

samarskite (Northrop, 1996). After the minerals have been classified into their appropriate groups, they must be further defined by their dominant component. In the Petaca samples analyzed, yittrium is the dominant A-site element, so the minerals are properly named as euxenite-(Y), samarskite-(Y), and polycrase-(Y).

Columbite

Samples of columbite [(Fe, Mn)(Nb, Ta)$_2$O$_6$] were collected and analyzed from 8 of the pegmatites during the search for Y-REE-Ta-Nb-Ti oxides. In some cases, the samples were simply "black oxides" that were suspected to be samarskite but turned out to be columbite or mixtures of columbite and samarskite. All the samples were higher in MnO than FeO, with MnO ranging from 6.8 to 16 wt% and FeO from <1 to 10 wt%. Likewise, Nb_2O_5 ranged from 32–73 wt% and Ta_2O_5 from 5.2-44 wt%. Therefore, all the samples are classified as columbite-(Mn), rather than tantalite. Samples from La Paloma and Alamos Canyon pegmatites provided the highest MnO and Ta_2O_5 examples, whereas samples from Globe exhibited the highest proportions of FeO and Nb_2O_5. Crystallization of columbite-tantalite in individual pegmatites demonstrates a trend of increasing MnO and Ta_2O_5 toward the interior (later) zones as pegmatite crystallization progresses (Cerny et al., 1985). Higher Ta/Nb and Mn/Fe ratios indicate a greater degree of evolution between zones within a pegmatite body and between bodies within a pegmatite field (Spilde and Shearer, 1992). Thus, based on the concentration of Ta, Nb, Mn, and Fe in our samples, La Paloma and Alamos Canyon are the most highly evolved of the 10 pegmatites sampled.

Origin of the Pegmatites

The origin of the Petaca District pegmatites is somewhat enigmatic. Granitic pegmatites are derived from fertile granites and are usually closely associated with their parental granitic intrusion (London, 2008; Jahns and Burnham, 1969). However, no such granite is present at Petaca. Two theories have been proposed for the genesis of the Petaca pegmatites. Jahns (1946) postulated that they were formed from late-stage crystallization of a volatile-rich granitic magma associated with a larger granite body that does not crop out in the area. The other theory, proposed by Gresens (1967), maintains that the pegmatites originated from a reaction of quartz and muscovite with an intergranular alkali-chloride fluid, and the REE and other rare elements were introduced by contamination from hydrothermal fluids. The explanation that the pegmatites are derived from a granitic magma is more supportable than Gresens' alternative theory for several reasons.

First, granitic pegmatites are classified on the basis of their composition, i.e., their geochemical signature, and from that, their origin can be determined (Cerny and Ercit, 2005). They are subdivided on the basis of their major minerals and minor elements. For example, one class of rare-element pegmatites (REL) may contain predominantly Be, Y, REE, U, Th, Nb>Ta and F and are in the REL-REE type classification. These pegmatites are thought to have formed at shallow depths and are found on the interior

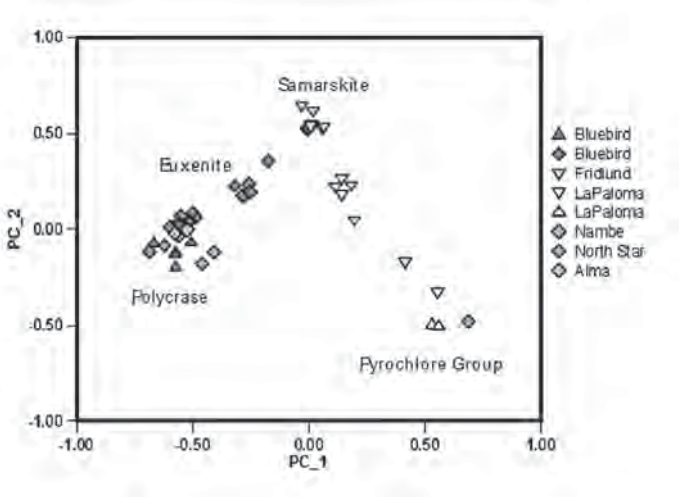

FIGURE 6. Plot of the scores for canonical variables 1 and 2 for the AB_2O_6 and ABO_4 minerals, using a three-group model of principle component analysis.

or the margin of their parental granites (Cerny and Ercit, 2005). Pegmatites may also be classed as petrogenic families, which include the LCT (**l**ithium, **c**esium, **t**antalum) and the NYF (**n**iobium, **y**ttrium and REE, **f**luorine) types (Cerny and Eric, 2005). These subdivisions speak mainly to the source lithologies of the parental granites, and to a certain extent, the tectonic affiliation of the pegmatites (Cerny, 1991). The LCT pegmatites are derived from substantially peraluminous granites of S-type (sedimentary-derived granite) or I-type (igneous protolith) granite or mixed S + I type. The NYF family, marked by Nb>Ta, Ti, Y, REE, Zr, U, Th, and F array of elements, are derived from sub- to metaluminous A-type (anorogenic) to I-type granites (Cerny and Ercit, 2005).

Secondly, the Petaca pegmatites, with their high Y- and Nb-bearing minerals, amazonitic K-spar, and common occurrence of fluorite as an accessory mineral, fall within the REL-REE class and the NYF type. This suggests that the pegmatites lie on the margin of a granitic body or bodies that are shallowly buried within the country rock of the district. Alternatively, a granite body may be nearby and covered by the extensive Cenozoic extrusives in the area.

CONCLUSION

This study has confirmed several minerals that are new for the Petatca district. We have discovered the presence of samarskite-(Y), polycrase-(Y), xenotime-(Y), and microlite, but more importantly, we have substantiated the high level of Nb and Y in these accessory minerals. Based on this, the Petaca pegmatites can be classified as members of the NYF type of pegmatites. The classification as REL-REE pegmatites and the NYF type support the supposition that the pegmatites are derived from A- or I-type granites and not from metasomatic activity as proposed by Gresens (1967).

ACKNOWLEDGMENTS

We appreciate the support and use of the electron microprobe, SEM and other facilities at Institute of Meteoritics/Department of Earth and Planetary Sciences, University of New Mexico. We thank Virgil Lueth and Penelope Boston for thoughtful reviews.

REFERENCES

Anders, E. and Grevesse, N., 1989, Abundances of the elements: Meteoritic and solar: Geochimica et Cosmochimica Acta, v. 53, p. 197-214.

Bingler, E. C., 1965, Precambrian geology of La Madera Quadrangle, Rio Arriba County, New Mexico: New Mexico Bureau Mines and Mineral Resources, Bulletin 80, 132 p.

Bingler, E. C., 1968, Geology and mineral resources of Rio Arriba County, New Mexico: New Mexico Bureau Mines and Mineral Resources, Bulletin 91, 158 p.

Cerny, P, 1991, Fertile granites of Precambrian rare-element granitic fields: Is geochemistry controlled by tectonic setting or source lithologies?: Precambian Research, v. 51, p. 429-468.

Cerny, P. and Ercit, T. S., 2005, The classification of granitic pegmatites revisited: Canadian Mineralogist, v. 43, p. 2005-2026.

Cerny, P., Meintzer, R.E., and Anderson, A.J., 1985, Extreme fractionation in rare-element granitic pegmatites: Selected examples of data and mechanisms: Canadian Mineralogist, v. 23, p. 381-421.

Chenoweth, W. L., 1974, Uranium in the Petaca, Ojo Caliente and Bromide Districts, Rio Arriba County, New Mexico: New Mexico Geological Society, 25th Field Conference Guidebook, p. 315.

Ercit, T. S., 2005, Identification and alteration trends of granitic-pegmatite-hosted (Y,REE,U,Th)-(Nb,Ta,Ti) oxide minerals: A statistical approach: Canadian Mineralogist, v. 43, p. 1291-1303.

Ewing, R.C., 1976, A numerical approach toward the classification of complex, orthorhombic, rare-earth, AB_2O_6-type Nb-Ta-Ti oxides: Canadian Mineralogist, v. 14, p. 111-119.

Goldstein, J.I., Newbury, D.E., Joy, D.C., Lyman, C.E., Echlin, P., Lifshin, E., Sawyer, L., and Michael, J., 2003, Scanning Electron Microscopy and X-Ray Microanalysis (3rd Ed): New York, Plenum Publishers, 689 p.

Gresens, R.L., 1967, Tectonic-hydrothermal pegmatites: II, An example: Contributions to Mineralogy and Petrology, v. 16, p. 1-28.

Heinrich, E. W., 1962, Radioactive Columbite: The American Mineralogist v. 47, p. 1363-1379.

Heinrich, E. W., Borup, R. A., and Levinson, A. A., 1960, Relationships between geology and composition of some pegmatitic monazites: Geochimica et Cosmochimica Acta, v. 19, p. 222-231.

Hess, F. L., and Wells, R. C., 1930, Samarskite from Petaca, New Mexico: American Journal of Science, 5th ser., v. 19, p. 17-26.

Holmes, J. A., 1899, Mica deposits in the United States: U.S. Geological Survey, 20th Annual Report, p. 691-707.

Jahns, R. H., 1946, Mica deposits of the Petaca District, Rio Arriba County, New Mexico: New Mexico Bureau Mines and Mineral Resources, Bulletin 25, 294 p.

Jahns, R. H., 1974, Structural and petrogenetic relationships of pegmatites in the Petaca District, New Mexico: New Mexico Geological Society, 25th Field Conference Guidebook, 371-375 p.

Jahns, R. H., and Burnham, C.W., 1969, Experimental studies of pegmatite genesis. Part I. A model for the derivation and crystallization of granitic pegmatites: Economic Geology, v. 64, p. 843-864.

Just, E., 1937, Geology and economic features of the pegmatites of Taos and Rio Arriba Counties, New Mexico: New Mexico Bureau Mines and Mineral Resources, Bulletin 13, 73 p.

Koning, D. J., Karlstrom, K., Salem, A., and Lombardi, C., 2007, Preliminary geologic map of the La Madera Quadrangle, Rio Arriba County, New Mexico: New Mexico Bureau of Geology and Mineral Resources, Open File Geologic Map-141, scale 1:12000.

London, D., 2008, Pegmatites: The Canadian Mineralogist Special Publication 10, Mineralogical Association of Canada, Quebec, Canada, 347 p.

Long, K. R., Van Gosen, B. S., Foley, N. K., and Cordier, D, 2010, The principal rare earth element deposits of the United States: U. S. Geological Survey Scientific Investigations Report 2010-5220, 96 p.

McLemore, V., North, R., and Leppert, S., 1988, REE, niobium, and thorium districts and occurrences in New Mexico: New Mexico Bureau of Mines and Mineral Resources, Open-File Report 324, 27 p.

Modreski, P. J., 1986, Radioactive minerals in pegmatites of Colorado and New Mexico, *in* Colorado pegmatites, abstracts, short papers, and field guides from the Colorado Pegmatite Symposium, May 30-June 2, 1986: Colorado Chapter, Friends of Mineralogy, Denver, Colorado, p. 37-45.

Northrop, S. A., 1959, Minerals of New Mexico: Albuquerque, University of New Mexico Press, 665 p.

Northrop, S. A., as revised by LaBruzza, F. A., 1996, Minerals of New Mexico, Albuquerque, University of New Mexico Press, 346 p.

Redmon, D. E, 1961, Reconnaissance of selected pegmatite districts in north-central New Mexico: U.S. Bureau of Mines, Information Circular 8013, 79 p.

Scott, A., Karlstrom, K, Koning, D., and Kempter, K., 2010, Preliminary geologic map of the La Tablas Quadrangle, Rio Arriba County, New Mexico: New Mexico Bureau of Geology and Mineral Resources, Open File Geologic Map-200, 1:12000.

Spilde, M.N. and Shearer, C.K., 1992, A comparison of tantalum-niobium oxide assemblages in two mineralogically distinct rare-element pegmatites, Black Hills, South Dakota: Canadian Mineralogist, v. 30, p. 719-737.

Sterrett, D. B., 1923, Mica deposits of the United States: U.S. Geological Survey Bulletin 740, p. 158-164.

Wells, R.C., 1928, Note on the J. Lawrence Smith method for the analysis of samarskite, American Chemical Soc. Journal, v.50, p.1017-1022

Wright, L. A., 1948, The Globe Pegmatite, Rio Arriba County, New Mexico: American Journal of Science, v. 246, no. 71, p. 655-688.

APPENDIX 1. Electron microprobe analyses of selected minerals from the Petaca Pegmatites.

Phase: Location:	Mnz Coats	Mnz Fridlund	Xeno Fridlund	Thorite Coats	Cher Coats	Thorite Fridlund	Poly Bluebird	Eux Bluebird	Smsk Fridlund	Mcl La Paloma
Oxides										
P_2O_5	28.58	27.92	33.39	7.23	14.45	3.05	0.03	0.00	0.06	0.00
As_2O_5	0.33	0.29	1.05	1.37	1.03	0.77	0.40	0.26	0.63	0.03
Nb_2O_5							27.45	42.54	39.70	6.48
Ta_2O_5							6.67	11.68	2.03	56.13
SiO_2	0.70	1.33	0.08	9.26	6.83	11.13	0.01	0.00	1.38	0.00
TiO_2							22.89	3.54	0.50	5.09
V_2O_3			0.00	2.88	2.44	2.32	0.07	0.03		
ZrO_2									0.25	0.01
ThO_2	9.57	7.35	0.39	53.37	47.73	72.18	2.98	2.25	1.82	0.11
UO_2	0.10	0.30	0.05	0.58	0.68	1.23	5.07	4.60	14.31	10.30
Al_2O_3	0.01	0.00	0.00	0.19	0.31	0.54	0.00	0.00	0.00	0.06
Y_2O_3	0.53	1.60	31.95	1.62	1.67	1.26	15.41	10.88	9.09	0.00
La_2O_3	9.02	11.84	0.00	0.04	0.00	0.07	0.03	0.00	0.06	0.00
Ce_2O_3	21.64	26.63	0.18	0.72	0.73	0.19	0.00	0.16	0.22	0.02
Pr_2O_3	2.45	2.73	0.06	0.09	0.03	0.10	0.05	0.04	0.00	0.10
Nd_2O_3	9.56	11.15	0.27	0.68	1.30	0.49	0.46	0.35	0.42	0.13
Sm_2O_3	6.87	3.51	0.85	1.25	1.50	0.27	0.79	0.69	0.50	0.17
Eu_2O_3	0.20	0.00	0.00	0.04	0.19	0.05	0.17	0.01	0.07	0.00
Gd_2O_3	4.57	1.10	5.93	1.91	1.99	0.54	2.18	1.50	2.09	0.14
Tb_2O_3	0.52	0.07	2.09	0.69	0.65	0.10	0.60	0.42	0.77	0.00
Dy_2O_3	1.56	0.96	15.54	4.84	4.08	0.66	4.35	2.74	7.33	0.00
Ho_2O_3	0.63	0.19	1.79	0.34	0.24	0.00	1.01	0.58	1.49	0.52
Er_2O_3	0.17	0.34	3.63	1.26	1.16	0.00	2.02	1.25	4.02	0.22
Tm_2O_3	0.09	0.16	0.30	0.01	0.42	0.00	0.34	0.00	0.69	0.00
Yb_2O_3	0.00	0.05	0.68	0.99	0.69	0.16	2.05	1.47	4.94	0.00
Lu_2O_3	0.00	0.06	0.12	0.28	0.07	0.05	0.74	0.38	0.75	0.00
MnO							0.18	1.12	0.41	0.54
FeO							1.02	5.97	0.46	0.69
CaO	1.56	0.55	0.02	2.74	5.14	1.62	0.40	4.04	2.71	9.69
Na2O							0.20	0.05	0.01	3.70
PbO	0.56	0.47	0.04	0.69	4.08	0.00	1.45	0.93	0.13	3.65
F	0.36	0.36	0.00	1.09	0.65	0.94	0.11	0.07	0.58	1.28
Total	99.41	98.81	98.42	93.71	97.78	97.70	99.10	97.54	97.41	99.04

APPENDIX 1. Continued.

Phase: Location:	Mnz Coats	Mnz Fridlund	Xeno Fridlund	Thorite Coats	Cher Coats	Thorite Fridlund	Poly Bluebird	Eux Bluebird	Smsk Fridlund	Mcl La Paloma
Cations										
P	0.971	0.951	0.999	0.327	0.572	0.145	0.001	0.000	0.0025	0.000
As	0.007	0.006	0.020	0.038	0.025	0.023	0.009	0.006	0.016	0.001
Nb							0.518	0.868	0.895	0.157
Ta							0.076	0.143	0.028	0.819
Si	0.028	0.053	0.003	0.495	0.319	0.628	0.000	0.000	0.069	0.000
Ti							0.719	0.120	0.019	0.205
V			0.000	0.124	0.092	0.105	0.002	0.001		
Zr									0.006	0.000
Th	0.087	0.067	0.003	0.649	0.508	0.926	0.028	0.023	0.021	0.001
U	0.001	0.003	0.000	0.007	0.007	0.015	0.047	0.046	0.159	0.123
Al	0.001	0.000	0.000	0.012	0.017	0.036	0.000	0.000	0.000	0.004
Y	0.011	0.034	0.601	0.046	0.042	0.038	0.343	0.261	0.241	0.000
La	0.134	0.176	0.000	0.001	0.000	0.001	0.001	0.000	0.001	0.000
Ce	0.318	0.392	0.002	0.014	0.013	0.004	0.000	0.003	0.004	0.000
Pr	0.036	0.040	0.001	0.002	0.000	0.002	0.001	0.001	0.000	0.002
Nd	0.137	0.160	0.003	0.013	0.022	0.010	0.007	0.006	0.008	0.003
Sm	0.095	0.049	0.010	0.023	0.024	0.005	0.011	0.011	0.009	0.003
Eu	0.003	0.000	0.000	0.001	0.003	0.001	0.003	0.000	0.001	0.000
Gd	0.061	0.015	0.069	0.034	0.031	0.010	0.030	0.022	0.035	0.002
Tb	0.007	0.001	0.024	0.012	0.010	0.002	0.008	0.006	0.013	0.000
Dy	0.020	0.013	0.177	0.083	0.062	0.012	0.059	0.040	0.118	0.000
Ho	0.008	0.002	0.020	0.006	0.004	0.000	0.013	0.008	0.024	0.009
Er	0.002	0.004	0.040	0.021	0.017	0.000	0.027	0.018	0.063	0.004
Tm	0.001	0.002	0.003	0.000	0.006	0.000	0.004	0.000	0.011	0.000
Yb	0.000	0.001	0.007	0.016	0.010	0.003	0.026	0.020	0.075	0.000
Lu	0.000	0.001	0.001	0.005	0.001	0.001	0.009	0.005	0.011	0.000
Mn							0.006	0.043	0.017	0.024
Fe							0.036	0.225	0.019	0.031
Ca	0.067	0.024	0.001	0.157	0.258	0.098	0.018	0.195	0.145	0.557
Na							0.016	0.004	0.001	0.385
Pb	0.006	0.005	0.000	0.010	0.051	0.000	0.016	0.011	0.002	0.053
F	0.046	0.046	0.000	0.176	0.094	0.160	0.015	0.010	0.090	0.206
Total	2.046	2.043	1.986	2.271	2.188	1.986	2.050	2.098	2.083	2.141

Abbreviations: Mnz, monazite; Xeno, xenotime; Cher, cheralite; Poly, polycrase; Eux, euxenite; Smsk, samarskite; Mcl, microlite.
Cations based on 4 oxygens

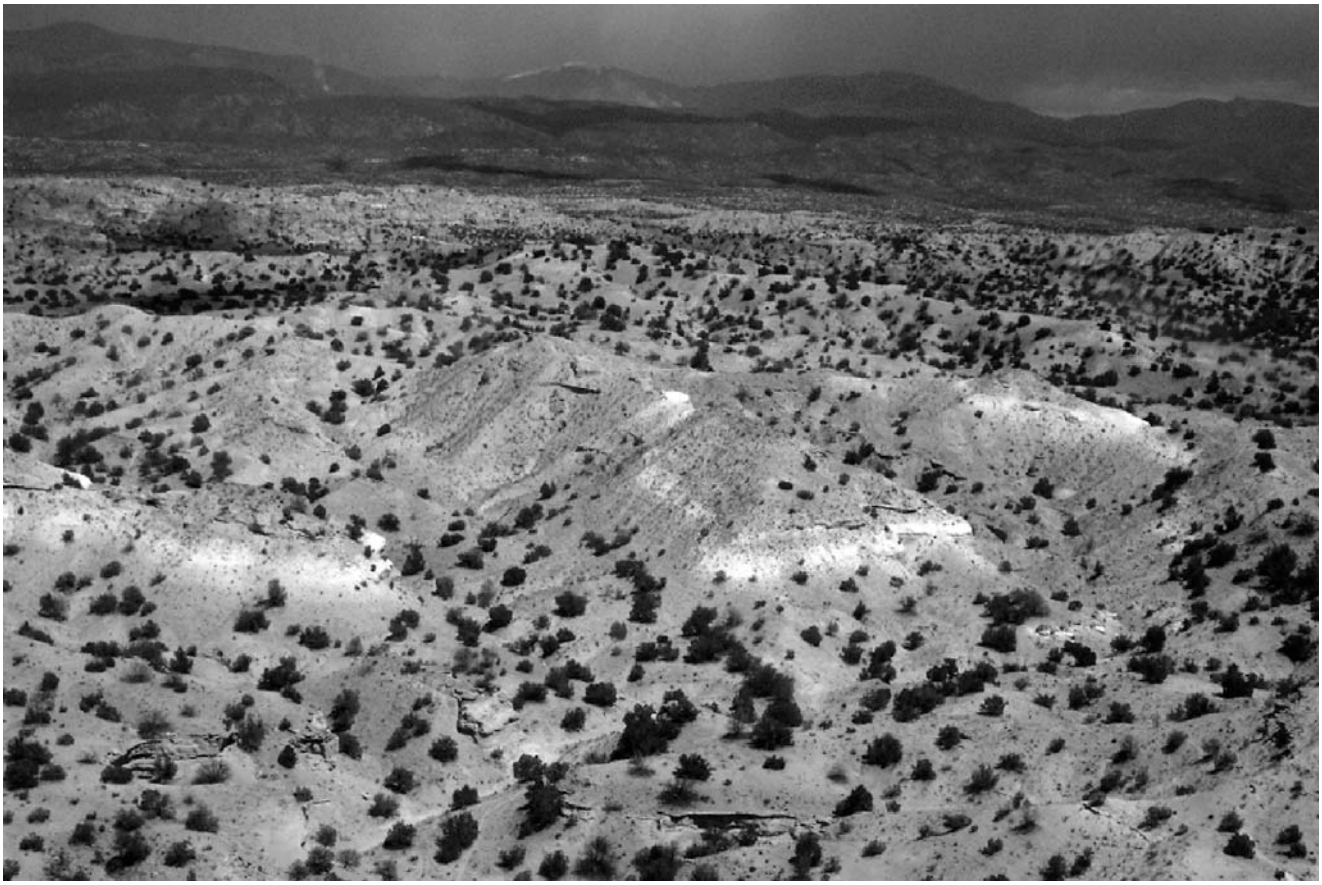

Photograph of badlands in the east-center Española Basin developed in the Tesuque Formation of the Santa Fe Group. The white band is a fine ash bed known as White Ash no. 3 (Galusha and Blick, 1971). In the distance lies the western front of the Sangre de Cristo Mountains, which is composed of Proterozoic granitic and metamorphic rocks. Two kilometers west of here is a north- to northwest-trending band of low-grade uranium mineralization. The uranium in this band was precipitated naturally in ground water and was ultimately sourced from rhyolitic ash beds, such as the White Ash no. 3, or from Proterozoic rocks in the Sangre de Cristo Mountains. Photograph courtesy of Dennis McQuillan.